Supporting Information

A novel regenerative hybrid composite adsorbent with improved removal capacity of lead ions in water

Melvin S. Samuel, Mingwei Shang, Stanislav Klimchuk, and Junjie Niu*

Department of Materials Science and Engineering, CEAS, University of Wisconsin-Milwaukee, Milwaukee, WI 53211, USA

*Corresponding author: niu@uwm.edu (JN)

Figures S1-8

Tables S1-8

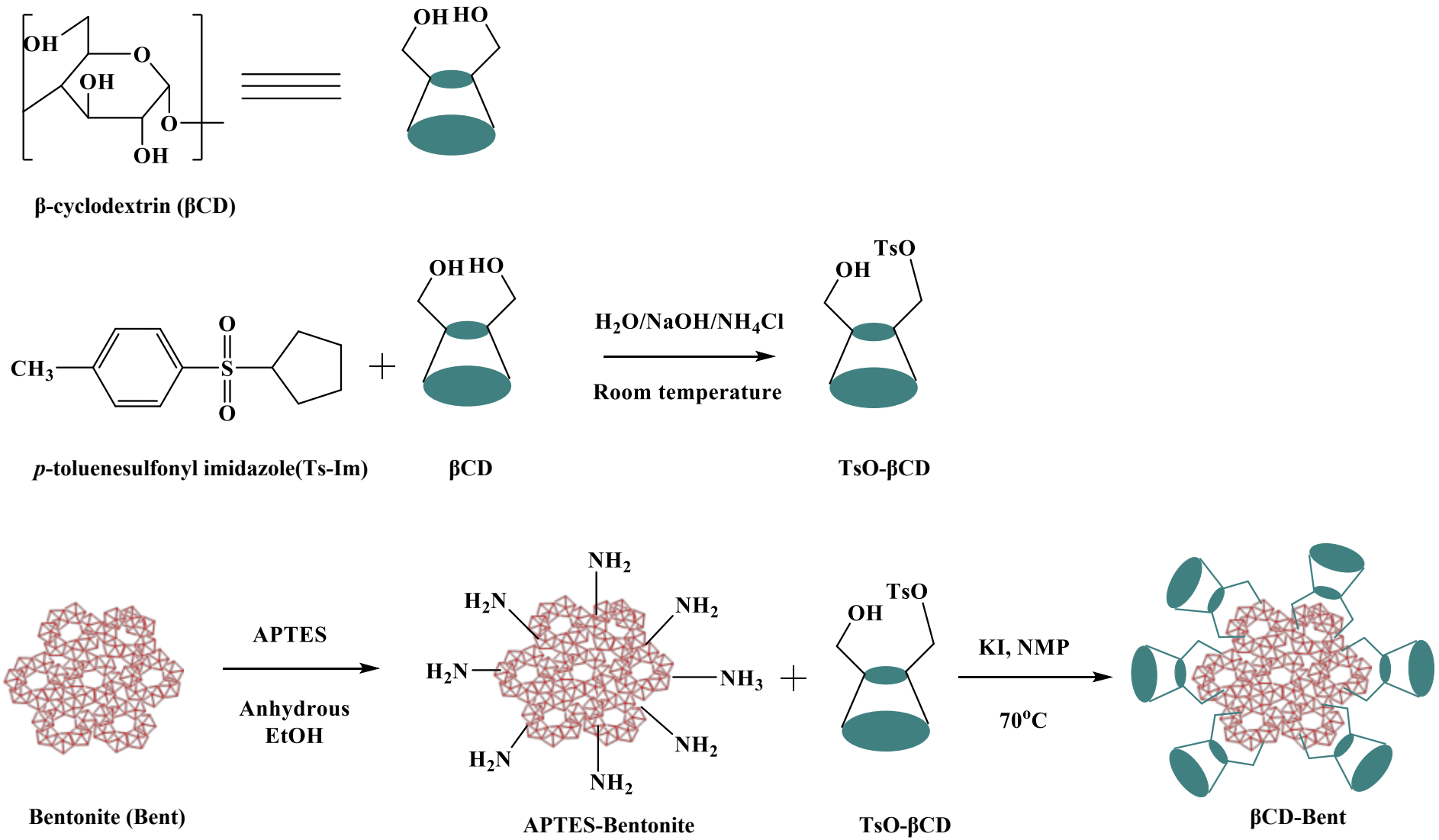

Figure S1. Synthesis of β-cyclodextrin functionalized bentonite (βCD-Bent).

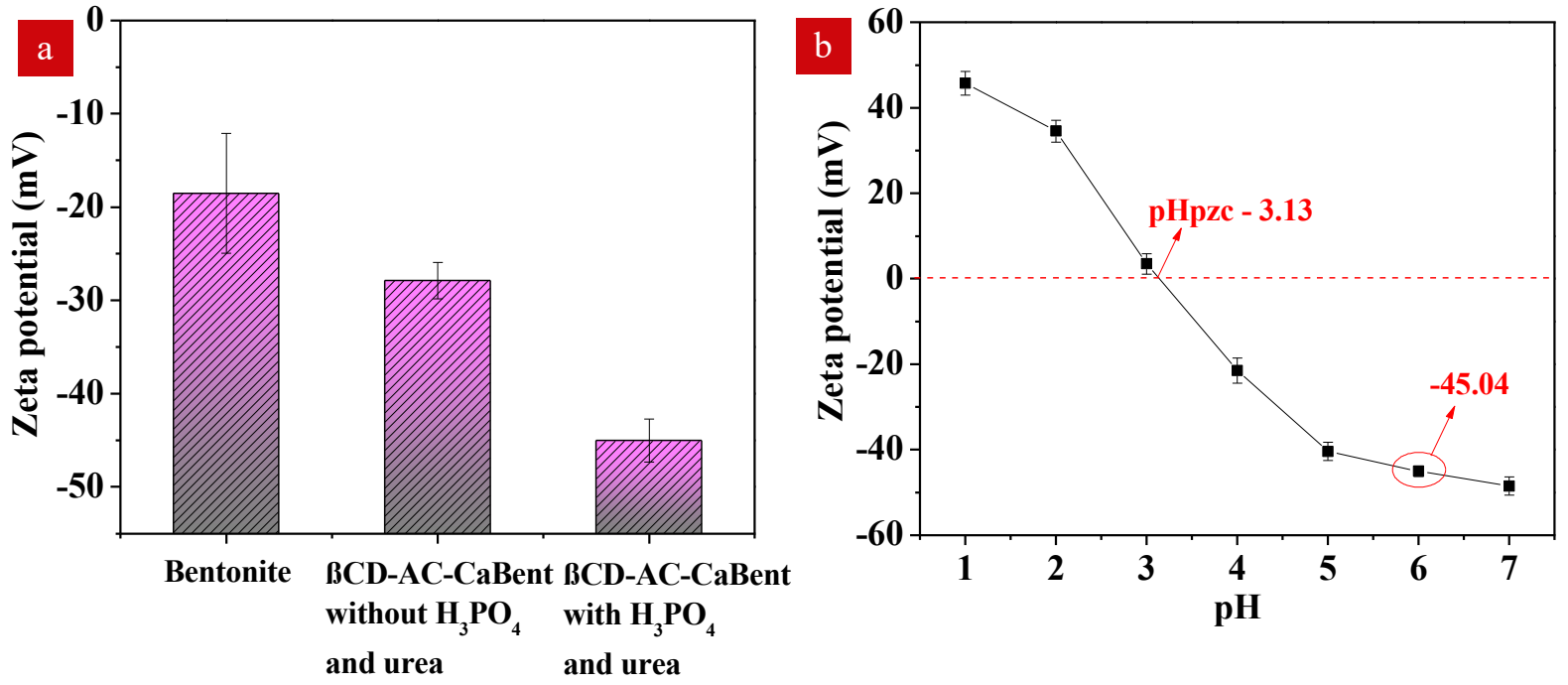

Figure S2. (a) Zeta potentials of bentonite and βCD-AC-CaBent before and after the treatments with H_3PO_4 and urea. (b) Zeta potential of the βCD-AC-CaBent at different pH values.

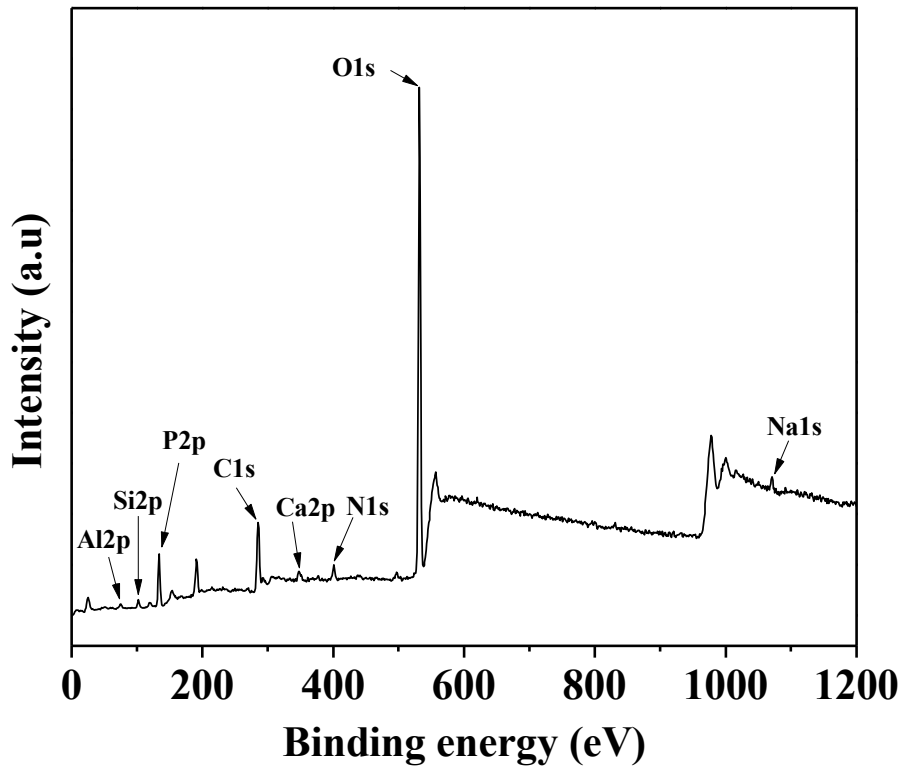

Figure S3. XPS spectrum survey of the obtained βCD-AC-CaBent adsorbent.

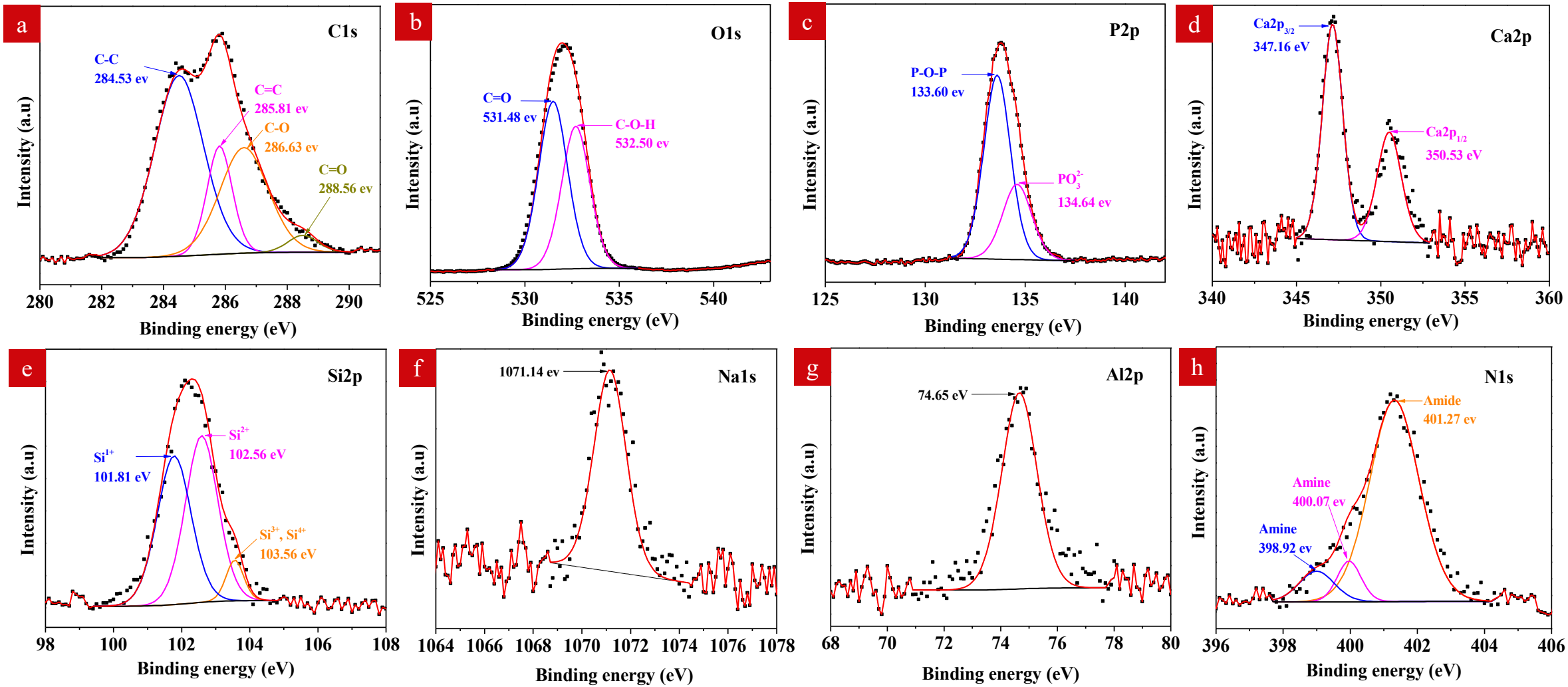

Figure S4. High-resolution XPS spectra of C1s (a), O1s (b), P2p (c), Ca2p (d), Si2p (e), Na1s (f), Al2p (g) and N1s (h) of the adsorbent.

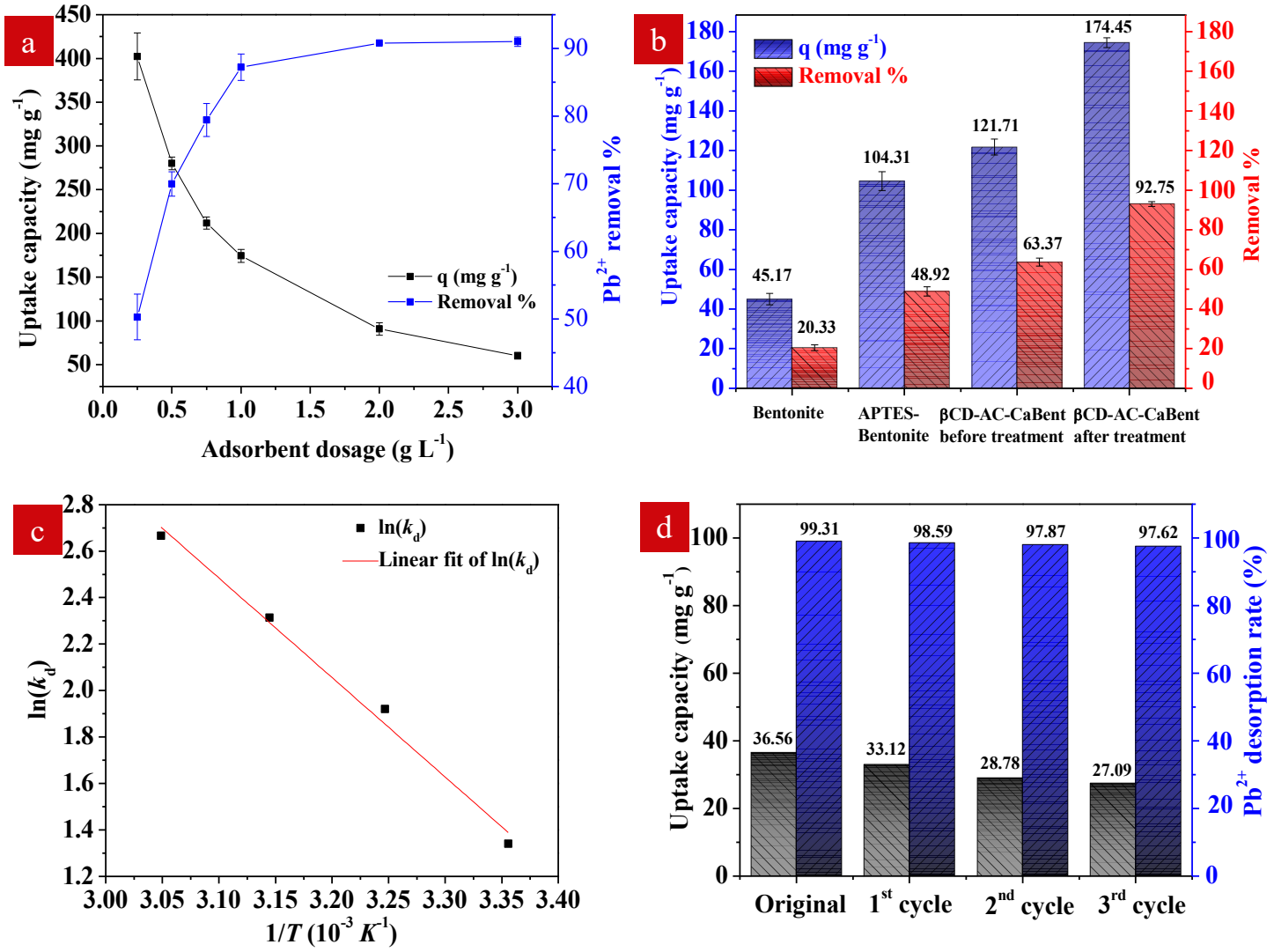

Figure S5. (a) Pb^{2+} adsorption uptake capacity and removal percentage of βCD-AC-CaBent with different adsorbent dosages at room temperature. pH: 6.0. Pb^{2+} concentrations: 200 mg L^{-1}. (b) Batch adsorption performance: Comparisons of bentonite, APTES-bentonite, βCD-AC-CaBent, βCD-AC-CaBent before and after treatments with H_3PO_4 and urea at pH 6.0. (c) Thermodynamic plot of $\ln(K_d)$ vs $1/T$ during the adsorption process, K_d is the distribution coefficient for adsorption. (d) Regeneration of βCD-AC-CaBent under continuous column adsorption. Pb^{2+} concertation: 50 mg L^{-1}; pH: 6.0; flow rate: 50 mL min^{-1}; bed height: 1.65 cm.

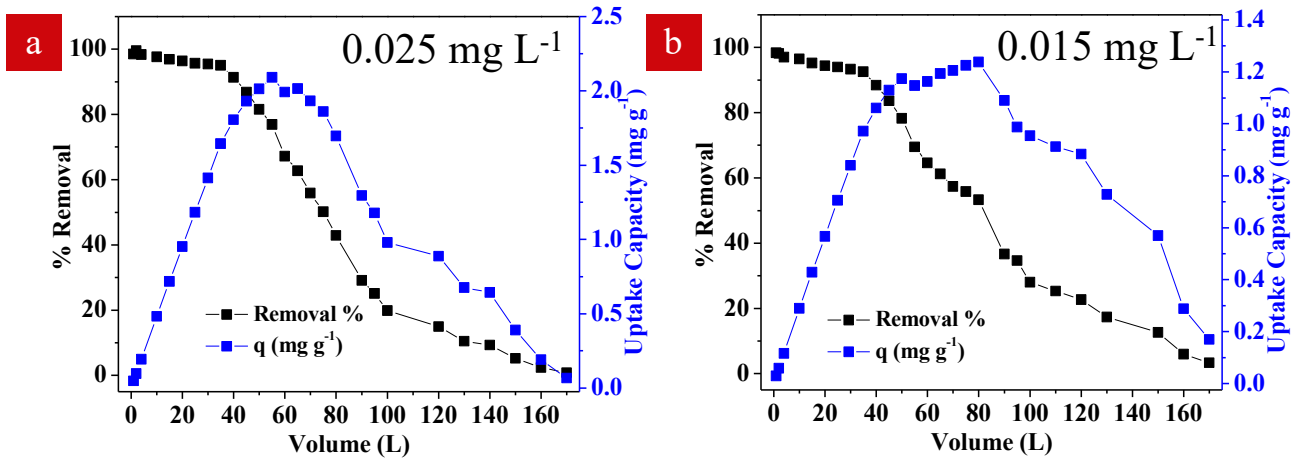

Figure S6. Removal % and uptake capacity of Pb^{2+} on βCD-AC-CaBent under low Pb^{2+} concentrations of 0.025 mg L^{-1} (a) and 0.015 mg L^{-1} (b), respectively. Adsorbent dosage: 0.5 g L^{-1}; pH: 6.0; flow rate: 50 mL min^{-1}.

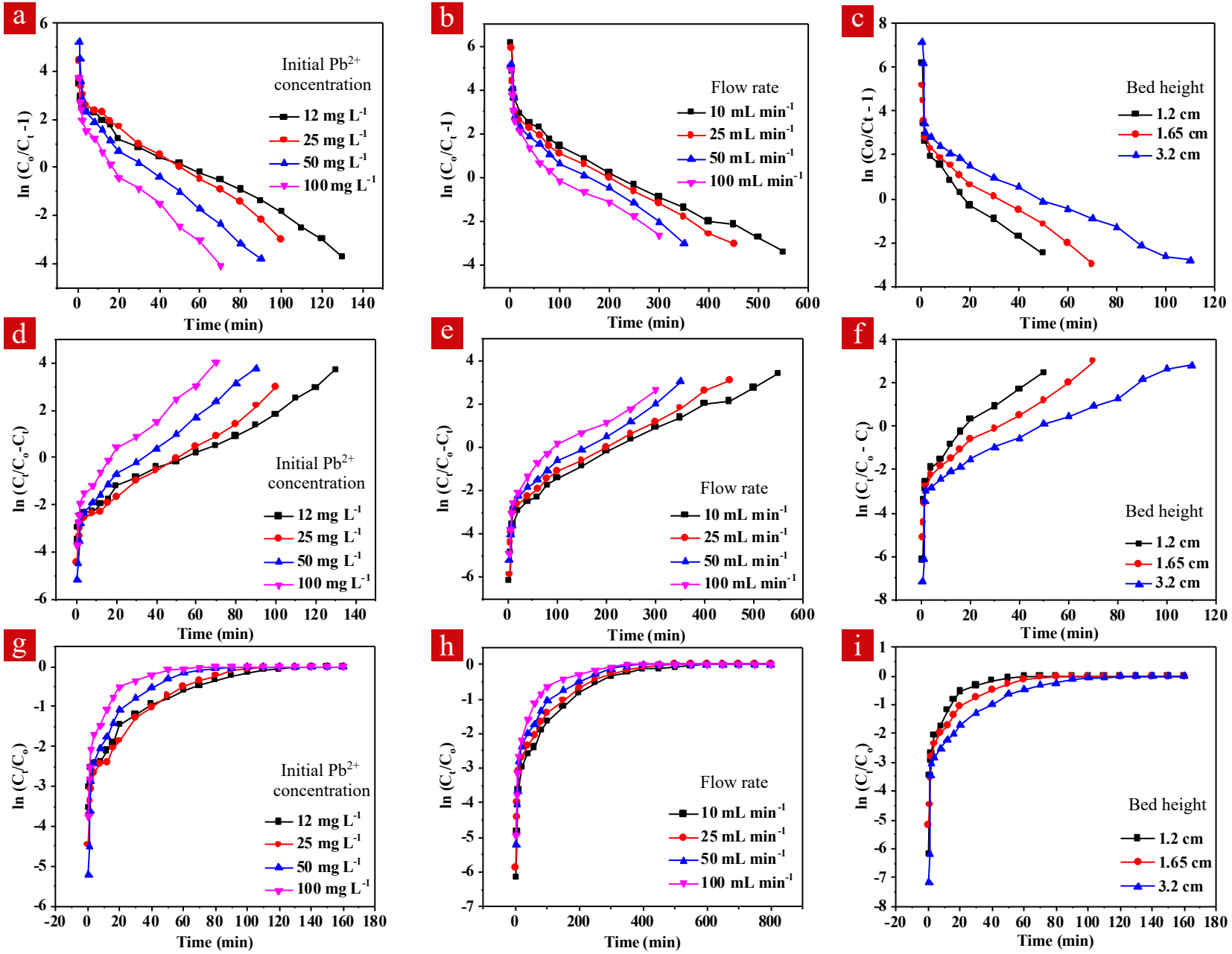

Figure S7. Linear representations of the adsorption on βCD-AC-CaBent in the models of Thomas (a, b, c), Yoon-Nelson (d, e, f), and Bohart-Adam (g, h, i) at different initial Pb^{2+} concentrations, flow rates and bed heights in the continuous column tests, respectively.

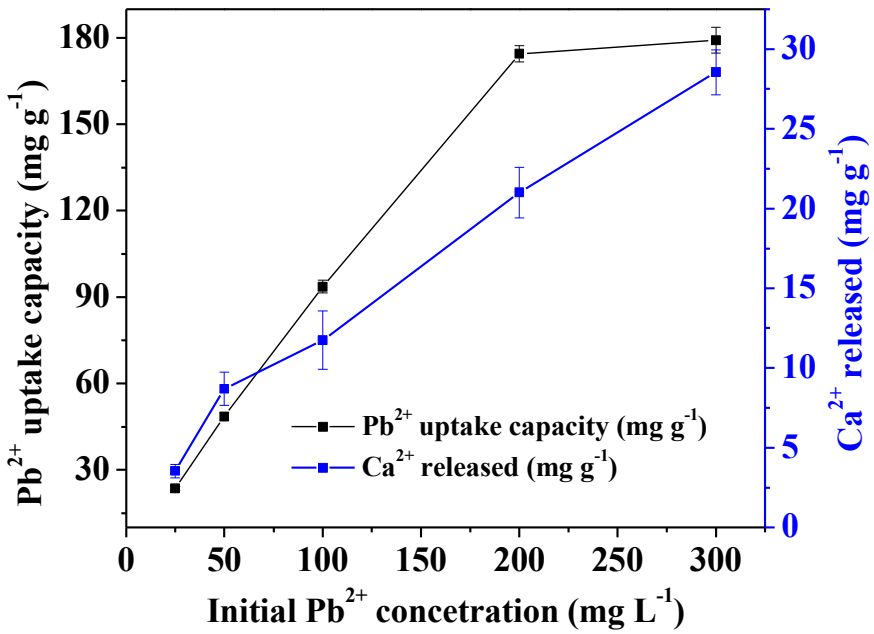

Figure S8. The Pb^{2+} uptake capacity and the corresponding released Ca^{2+} concentration at varying Pb^{2+} concentrations.

Table S1. EDX elemental analysis of pure bentonite (a) and βCD-AC-CaBent (b) adsorbents.

a

Element	% Weight	% Atomic
Sodium	0.529	0.322
Calcium	0.927	0.323
Aluminium	0.089	0.046
Silicon	0.548	0.273
Carbon	46.185	53.803
Oxygen	51.718	45.230

b

Element	% Weight	% Atomic
Sodium	0.073	0.043
Calcium	2.921	1.004
Aluminium	0.079	0.034
Silicon	7.063	3.464
Carbon	65.881	75.559
Oxygen	21.812	18.780

Table S2. Kinetics parameters of the Pb^{2+} adsorption on βCD-AC-CaBent using different models.

Concentration (mg L^{-1})	**Experimental q_e (mg g^{-1})**	**pseudo-first-order**			**pseudo-second-order**			**Intraparticle diffusion**		
		K_1 (min^{-1})	q_e (mg g^{-1})	R^2	K_2 (min^{-1})	q_e (mg g^{-1})	R^2	R_i	C	R^2
25	23.57	0.019	12.02	0.779	0.167	24.88	0.986	1.336	8.186	0.887
50	48.75	0.019	31.65	0.971	0.393	49.50	0.998	3.194	11.214	0.884
100	96.66	0.023	70.65	0.992	0.237	98.04	0.992	6.255	19.328	0.942
200	174.45	0.024	137.87	0.946	0.220	175.43	0.991	10.997	29.674	0.933

Table S3. Equilibrium isotherm parameters for the Pb^{2+} adsorption on βCD-AC-CaBent.

Experimental		**Isotherm model**					
Adsorbent dosage (g L^{-1})	q_e (mg g^{-1})	Langmuir			Freundlich		
		q_{max} (mg g^{-1})	K_L (L mg^{-1})	R^2	K_f (mg g^{-1})	N	R^2
0.25	402.20	434.78	0.060	0.950	65.70	2.69	0.949
0.50	279.86	303.03	0.077	0.907	42.52	2.39	0.966
0.75	211.80	212.76	0.162	0.928	41.91	2.59	0.970
1.00	174.45	175.44	0.548	0.985	53.76	2.85	0.992
2.00	90.78	91.74	0.602	0.974	30.29	2.81	0.991
3.00	60.32	60.97	1.146	0.985	24.66	3.09	0.964

Table S4. Comparison of adsorption performance of different adsorbents.

Adsorbent	Adsorption capacity (mg g^{-1})	Experimental condition							Model		References
		Adsorbent dosage (g L^{-1})	Initial Pb^{2+} concentration mg L^{-1}	Temperature (°C)	pH	Reaction time (h)	Analysis method	Desorption method	Kinetics	Adsorption isotherm	
Plasma- treated activated carbon	2.15	1.00	20	25	N/A	24	ICP-OES	HNO_3	pseudo-first order	Langmuir	[1]
Treated activated carbon	29.44	1.00	5-70	37±2	5.0	20	ICP-OES	HNO_3	N/A	Langmuir	[2]
EDTA-reduced graphene oxides	228.00	0.01-0.02	5-300	25±1	6.8	24	AAS & ICP-OES	HCl	N/A	Langmuir	[3]
Carbon nitride	65.60	0.02-0.90	10	45	6.0	24	Chlorophosphonazo III spectrometric technique at 616 nm	HCl	pseudo-second order	Langmuir	[4]
Phosphorylated cellulose microsphere	108.50	1.00	100	25, 40 & 60	5.0	0.5	AAS	HCl	pseudo-second order	Langmuir	[5]
Mesoporous silica (POH-MS)	272	0.01	100	22	4.8	2	AAS	HCl	pseudo-second order	Langmuir	[6]
Activated alumina	83.33	1.0-10.0	10-800	Room temperature	5.0	2	AAS	N/A	pseudo-second order	Langmuir	[7]
β-cyclodextrin polymers	196.40	0.05	1-200	25	5.0	24	AAS	HNO_3	pseudo-second order	Freundlich	[8]
βCD-AC-CaBent	**434.78**	**1.0, 2.0, 3.0**	**25-300**	**Room temperature**	**6.0**	**1.00**	**ICP-MS, AAS**	**HCl**	**pseudo-second order**	**Langmuir, Freundlich**	**This study**

Table S5. Thermodynamics properties of Pb^{2+} removal on βCD-AC-CaBent.

Initial Pb^{2+} concentration ($mg\ L^{-1}$)	T ($1/K$)	$\ln(k_d)$	ΔG^o ($kJ\ mol^{-1}$)	ΔH^o ($kJ\ mol^{-1}$)	ΔS^o ($J\ mol^{-1}K^{-1}$)	R^2
200	298	1.640	-4.062	35.618	131.071	0.9912
	308	1.921	-4.919			
	318	2.197	-5.809			
	328	2.666	-7.270			

Table S6. Experimental parameters of breakthrough curves with Pb^{2+} adsorption on βCD-AC-CaBent under different conditions at room temperature and pH 6.

	C_o (mg L^{-1})	Flow rate (mL min^{-1})	Bed height (cm)	M (g)	t_b (min)	V_b (mL)	q_b (mg g^{-1})	t_s (min)	V_s (mL)	q_s (mg g^{-1})	t_o (min)	U_z (cm min^{-1})	$HMTZ$ (cm)	q_{max} (mg g^{-1})
Initial Pb^{2+} concentration (mg L^{-1})	12	50	1.65	1.5	16	800	8.40	130	6500	9.33	114	0.014	1.446	18.59
	25	50	1.65	1.5	12	600	13.85	85	4500	10.00	78	0.019	1.430	20.38
	50	50	1.65	1.5	8	300	16.77	65	3250	14.15	59	0.025	1.497	29.74
	100	50	1.65	1.5	1.5	75	20.85	45	2250	19.20	43.5	0.036	1.595	33.26
Flow rate (mL min^{-1})	50	10	1.65	1.5	65	650	27.62	470	4700	15.66	405	0.003	1.421	39.78
	50	25	1.65	1.5	18	450	22.06	150	3750	12.75	132	0.011	1.452	36.56
	50	50	1.65	1.5	6	300	16.77	65	3250	9.33	59	0.025	1.497	29.74
	50	100	1.65	1.5	1.5	150	10.92	27	2700	12.58	25.5	0.061	1.550	21.74
Bed height (cm)	50	50	1.20	1.0	3	150	16.78	45	2250	16.71	42	0.026	1.120	26.09
	50	50	1.65	1.5	6	300	16.00	65	3250	14.15	59	0.025	1.490	29.74
	50	50	3.20	3.0	10	500	13.91	95	4750	9.36	85	0.033	2.860	21.97

t_b – 10% break through time (min)
V_b – breakthrough volume (mL)
q_b – uptake capacity at breakthrough time (min)
t_s – 90% saturation time (min)
V_s – saturation volume (mL)
t_δ – time require for the movement of the mass transfer zone (min)
U_z – mass transfer zone (MTZ) moving rate (cm min^{-1})
HMTZ - Height of MTZ (cm)
q_{max} - experimental uptake capacity (mg g^{-1})

Table S7. Comparison of the adsorption performance of the βCD-AC-CaBent and other adsorbents in a fixed bed column.

Adsorbent	Experimental condition							Fitting column model	Uptake capacity ($mg\ g^{-1}$)	References
	Flow rate ($mL\ min^{-1}$)	Adsorbent dosage (g)	Initial Pb^{2+} concentration ($mg\ mL^{-1}$)	pH	Bed height (cm)	Analysis method	Regeneration			
Amberlite IRC-718 chelating resin	1, 3	N/A	0.375	5.6	N/A	AAS	1 M HNO_3 .	N/A	19.90	[9]
Chelex-100	2	N/A	0.375	5.6	N/A	AAS	1 M HNO_3	N/A	22.80	[9]
Coir fibres	40	100	2.13, 3.21, 4.16	N/A	N/A	AAS	0.025 M NaOH	N/A	16.60	[10]
Carbonaceous material and activated carbon	5	1.4, 2.9, 7.7 of carbonaceous material and 0.7, 1.9, 3.9 g of activated carbon	20	6.0	4-8	AAS	N/A	N/A	9.10	[11]
Olive stone treated by H_2SO_4	6	5	10-150	5	4.4	AAS	N/A	Thomas, Yoon-Nelson, Bohart-Adam and Dose response	1.31	[12]
Phosphorylated cellulose microsphere	1, 1.4, 3	0.3 – 0.6	50, 100, 150	3.0, 4.0, 5.0	5, 7.5, 10	AAS	0.1 M HNO_3	Thomas, Yoon−Nelson, Bohart-Adam, BDST, Dose Response	144.95	[5]
Modified beer lees	1, 3, 6	4, 8, 12 g	15, 30, 60	4.0	3, 6, 9	ICP–OES	N/A	Thomas, Yoon–Nelson and BDST	29.60	[13]
Laterite	10, 15, 20	N/A	3, 9, 15	N/A	2, 5, 7	AAS	N/A	Thomas, Yoon-Nelson and Bohart-Adam	5.43	[14]
βCD-AC-CaBent	**10, 25, 50, 100**	**1.0, 1.5, 2.0**	**12, 25, 50, 100**	**6.0-7.0**	**1.25, 1.65, 3.2**	**ICP-MS and AAS**	**0.1 M HCl**	**Thomas, Yoon-Nelson and Bohart-Adam**	**39.78**	**This study**

Table S8. Thomas, Yoon-Nelson and Bohart-Adam model parameters with various initial Pb^{2+} concentrations, flow rates, and bed heights.

Model	**Parameter**	**Initial Pb^{2+} concentration C_o, mg L^{-1} (flow rate = 50 mL min^{-1})**				**Flow rate, mL min^{-1} (C_o = 50 mg L^{-1})**				**Bed height, cm (C_o = 50 mg L^{-1}; flow rate = 50 mL min^{-1})**		
Thomas		12	25	50	100	10	25	50	100	1.2	1.6	3.2
	R^2	0.9796	0.9504	0.9113	0.9361	0.9021	0.8947	0.8932	0.7967	0.7297	0.8872	0.8195
	K_{TH} (L mg^{-1} min^{-1})	0.003	2.46×10^{-3}	1.66×10^{-3}	9.84×10^{-4}	2.78×10^{-4}	7.9×10^{-4}	1.88×10^{-3}	4.51×10^{-3}	2.606×10^{-3}	1.89×10^{-3}	1.33×10^{-3}
	q_o (mg g^{-1})	22.65	43.70	64.89	76.92	87.91	74.32	58.25	44.71	61.20	58.42	47.10
Yoon-Nelson	R^2	0.9796	0.9504	0.9113	0.9361	0.9021	0.8947	0.8932	0.7967	0.7927	0.8872	0.8195
	K_{YN} (min)	0.0475	0.0617	0.0830	0.0948	0.0139	0.0395	0.0941	0.2556	0.1303	0.0949	0.0669
	τ (min)	56.29	52.45	38.93	23.95	263.38	89.18	34.95	13.45	24.48	34.05	56.52
Bohart-Adam	R^2	0.8425	0.8420	0.6666	0.6647	0.6976	0.6906	0.6917	0.6311	0.5678	0.6836	0.6002
	K_{BA} (L mg^{-1} min^{-1})	1.96×10^{-3}	1.61×10^{-3}	8.78×10^{-4}	4.07×10^{-4}	1.64×10^{-4}	4.74×10^{-3}	1.12×10^{-3}	2.99×10^{-3}	1.61×10^{-3}	1.14×10^{-3}	8.4×10^{-4}
	No (mg L^{-1})	21913	33004	59030	92430	72204	60667	47535	34221	54307	47427	37803

References

[1] C. Du, H. Liu, M. Xiao, D. Gao, D. Huang, Z. Li, T. Chen, J. Mo, K. Wang, C. Zhang, Adsorption of iron and lead ions from an aqueous solution by plasma-modified activated carbon, Ind. Eng. Chem. Res. 51 (2012) 15618–15625.
[2] J. Goel, K. Kadirvelu, C. Rajagopal, V.K. Garg, Removal of lead(II) by adsorption using treated granular activated carbon: Batch and column studies, J. Hazard. Mater. 125 (2005) 211–220.
[3] C.J. Madadrang, H.Y. Kim, G. Gao, N. Wang, J. Zhu, H. Feng, M. Gorring, M.L. Kasner, S. Hou, Adsorption behavior of EDTA-graphene oxide for Pb (II) removal, ACS Appl. Mater. Interfaces. 4 (2012) 1186–1193.
[4] R. Hu, X. Wang, S. Dai, D. Shao, T. Hayat, A. Alsaedi, Application of graphitic carbon nitride for the removal of Pb(II) and aniline from aqueous solutions, Chem. Eng. J. 260 (2015) 469–477.
[5] X. Luo, J. Yuan, Y. Liu, C. Liu, X. Zhu, X. Dai, Z. Ma, F. Wang, Improved Solid-Phase Synthesis of Phosphorylated Cellulose Microsphere Adsorbents for Highly Effective Pb2+ Removal from Water: Batch and Fixed-Bed Column Performance and Adsorption Mechanism, ACS Sustain. Chem. Eng. 5 (2017) 5108–5117.
[6] C. Gunathilake, M.S. Kadanapitiye, O. Dudarko, S.D. Huang, M. Jaroniec, Adsorption of Lead Ions from Aqueous Phase on Mesoporous Silica with P-Containing Pendant Groups, ACS Appl. Mater. Interfaces. 7 (2015) 23144–23152. doi:10.1021/acsami.5b06951.
[7] T.K. Naiya, A.K. Bhattacharya, S.K. Das, Adsorption of Cd(II) and Pb(II) from aqueous solutions on activated alumina, J. Colloid Interface Sci. 333 (2009) 14–26.
[8] J. He, Y. Li, C. Wang, K. Zhang, D. Lin, L. Kong, J. Liu, Rapid adsorption of Pb, Cu and Cd from aqueous solutions by β-cyclodextrin polymers, Appl. Surf. Sci. 426 (2017) 29–39.
[9] M.E. Malla, M.B. Alvarez, D.A. Batistoni, Evaluation of sorption and desorption characteristics of cadmium, lead and zinc on amberlite IRC-718 iminodiacetate chelating ion exchanger, Talanta. 57 (2002) 277–287.
[10] S.R. Shukla, R.S. Pai, Comparison of Pb(II) uptake by coir and dye loaded coir fibres in a fixed bed column, J. Hazard. Mater. 125 (2005) 147–153.
[11] E. Gutierrez-Segura, A. Colin-Cruz, C. Fall, M. Solache-Rios, P. Balderas-Hernández, Comparison of Cd-Pb adsorption on commercial activated carbon and carbonaceous material from pyrolysed sewage sludge in column system, Environ. Technol. 30 (2009) 455–461.
[12] M.C. De Hoces, G. Blázquez García, A.R. Gálvez, M.Á. Martín-Lara, Effect of the acid treatment of olive stone on the biosorption of lead in a packed-bed column, Ind. Eng. Chem. Res. 49 (2010) 12587–12595.
[13] Y. Dong, H. Lin, Competitive adsorption of Pb(II) and Zn(II) from aqueous solution by modified beer lees in a fixed bed column, Process Saf. Environ. Prot. 111 (2017) 263–269.
[14] S. Chatterjee, S. Mondal, S. De, Design and scaling up of fixed bed adsorption columns for lead removal by treated laterite, J. Clean. Prod. 177 (2018) 760–774.